ISPRS Journal of Photogrammetry and Remote Sensing 148 (2019) 208–220

Contents lists available at ScienceDirect

ISPRS Journal of Photogrammetry and Remote Sensing

journal homepage: www.elsevier.com/locate/isprsjprs

Variation of leaf angle distribution quantified by terrestrial LiDAR in natural European beech forest

Jing Liu[a,b,*], Andrew K. Skidmore[a,c], Tiejun Wang[a], Xi Zhu[a], Joe Premier[d], Marco Heurich[d,e], Burkhard Beudert[d], Simon Jones[b]

[a] Faculty of Geo-Information Science and Earth Observation (ITC), University of Twente, the Netherlands
[b] School of Sciences, RMIT University, Australia
[c] Department of Environmental Science, Macquarie University, Australia
[d] Department of Nature Protection and Research, Bavarian Forest National Park, Germany
[e] Chair of Wildlife Ecology and Management, University of Freiburg, Germany

ARTICLE INFO

Keywords:
Leaf inclination
Leaf inclination distribution function
Leaf angle distribution
Variation
Terrestrial laser scanning
Canopy structure
European beech

ABSTRACT

Leaf inclination angle and leaf angle distribution (LAD) are important plant structural traits, influencing the flux of radiation, carbon and water. Although leaf angle distribution may vary spatially and temporally, its variation is often neglected in ecological models, due to difficulty in quantification.

In this study, terrestrial LiDAR (TLS) was used to quantify the LAD variation in natural European beech (*Fagus Sylvatica*) forests. After extracting leaf points and reconstructing leaf surface, leaf inclination angle was calculated automatically. The mapping accuracy when discriminating between leaves and woody material was very high across all beech stands (overall accuracy = 87.59%). The calculation accuracy of leaf angles was evaluated using simulated point cloud and proved accurate generally ($R^2 = 0.88$, $p < 0.001$; RMSE = 8.37°; nRMSE = 0.16). Then the mean (θ_{mean}), mode (θ_{mode}), and skewness of LAD were calculated to quantify LAD variation.

Moderate variation of LAD was found in different successional status stands ($\theta_{mean} \in [36.91°, 46.14°]$, $\theta_{mode} \in [17°, 43°]$, skewness $\in [0.07, 0.48]$). Rather than the previously assumed spherical distribution or reported planophile distribution, here we find that LAD tended towards a uniform distribution in young and medium stands, and a planophile distribution in mature stands. A strong negative correlation was also found between plot θ_{mean} and plot median canopy height, making it possible to estimate plot specific LAD from canopy height data.

Larger variation of LAD was found on different canopy layers ($\theta_{mean} \in [33.64°, 52.97°]$, $\theta_{mode} \in [14°, 64°]$, skewness $\in [-0.30, 0.71]$). Beech leaves grow more vertically in the top layer, while more obliquely or horizontally in the middle and bottom layer.

LAD variation quantified by TLS can be used to improve leaf area index mapping and canopy photosynthesis modelling.

1. Introduction

Leaf angle is an important plant structural trait. It influences light interception and radiation scattering in the canopy, as well as the flux of carbon and water (Weiss et al., 2004). Therefore, it has been used as a parameter in canopy photosynthesis modelling (Tol et al., 2009), rainfall interception modelling (Xiao et al., 2000), and leaf area index (LAI) estimation. For individual leaves, leaf angle consists of leaf inclination angle and leaf azimuth angle. For the whole canopy, leaf angle distribution (LAD) is used to describe the probability of all leaves orientating at different directions. It is defned as the probability of leaf-normal falling within a unit interval of inclination angle. Usually a uniform azimuth direction can be assumed for most species (Ross, 1981; Falster and Westoby, 2003).

Due to measurement challenges, LAD is usually simplified using predefined mathematical functions, without considering its variation (Welles, 1990; Richardson et al., 2009; Tang et al., 2014). Six commonly used functions are depicted in Fig. 1. Planophile canopies are dominated by horizontal leaves, while erectophile canopies by vertical leaves (Lemeur and Blad, 1975). The spherical distribution (de Wit, 1965) is the most widely used due to its simplicity in calculating the leaf projection function value (approximated as 0.5 in any direction).

However, such simplification fails to consider the variation of LAD. In reality, LAD may vary for different species of plants (Pisek et al.,

* Corresponding author.

https://doi.org/10.1016/j.isprsjprs.2019.01.005
Received 14 May 2018; Received in revised form 29 December 2018; Accepted 8 January 2019

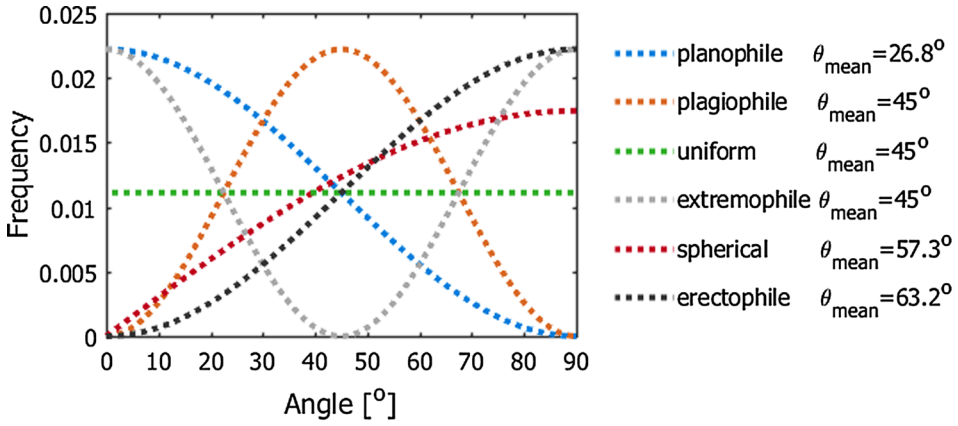

Fig. 1. Six predefined mathematical functions used to approximate leaf angle distribution and the corresponding average leaf inclination angle.

2013). Even for the same species, LAD may also exhibit a spatial and temporal variability. LAD was found to vary in different canopy layers in a tropical forest (Wirth et al., 2001), and several temperate deciduous trees (Raabe et al., 2015). LAD may also change with light exposure (McMillen and McClendon, 1979; Utsugi et al., 2006), time of the day (Shell et al., 1974) and season (Hosoi and Omasa, 2009; Raabe et al., 2015). Due to over-simplification, LAD has become one of the most poorly constrained radiative transfer model parameters (Ollinger, 2011). There is great potential to improve canopy photosynthesis modelling and LAI mapping if the LAD variation can be quantified.

One strategy to quantify leaf angle distribution is the direct geometrical approach. The basic principle is to obtain a representative description of the whole canopy by observations on individual leaf (Norman and Campbell, 1989), for example using compass and inclinometers (Ross, 1981). But direct contact often leads to disturbance of the leaves (Zheng and Moskal, 2012). The spatial coordinate apparatus (Lang, 1973) method was proposed to avoid direct contact, but the required number of leaves takes a large logistical effort to measure in forests. Consequently, the digital canopy photography method has been introduced (Ryu et al., 2010; Pisek et al., 2011). In this method, the authors first took several photos around the canopy at different heights. Then leaves were visually identified from each photo and each leaf angle was calculated using image processing (Pisek et al., 2011). Although this digital canopy photography method is robust and low-cost, it involves substantial user interaction when identifying individual leaves. In addition, taking photos for trees higher than 2 m would be very difficult in natural forests.

Another strategy to quantify leaf angle distribution (LAD) is the indirect radiometric approach. This approach yields a statistical estimate of LAD on plot level, rather than measuring the orientation of an individual leaf (Biskup et al., 2007). The basic principle is to record how radiation is attenuated by the canopy in several zenith directions, then one can invert the Beer's law for radiation interception to infer LAD (Norman and Campbell, 1989; Chen et al., 1991; Wagner and Hagemeier, 2006). However, this method has two main shortcomings. First, it cannot distinguish leaf and woody material. What was retrieved is the plant angle distribution rather than LAD (Chen et al., 1991). Second, the radiometric method makes assumptions (flat topography and homogenous tree height) which may not hold in heterogeneous natural forests.

With the development of close range remote sensing, efforts were made using three dimensional (3D) point cloud data to quantify canopy structure (Coops et al., 2007; Hancock et al., 2014; Calders et al., 2015). Magnetic 3D digitizer (Sinoquet et al., 1998; Falster and Westoby, 2003; Sinoquet et al., 2007), film-based stereo photogrammetry (Ivanov et al., 1995) and digital stereo imaging (Biskup et al., 2007) have been used to obtain 3D reconstructions of plants. But the drawback of these methods is their restricted usage to the outer canopy of small stands, usually an area of a few square meters (Muller-Linow et al., 2015). When combined with unmanned aerial vehicles (UAV), it can sample larger areas at stand scale. However, UAV-mounted cameras are vulnerable to lens distortion and image noise (McNeil et al., 2016).

From the 1990s, terrestrial LiDAR (TLS) has received increasing attention in vegetation surveys due to its capability to capture unprecedented detail of plant 3D structure, from individual tree to plot scale (Liang et al., 2018). With high pulse frequency and small beam divergence, tree trunks, branches, and even leaves can be easily recorded (Eitel et al., 2010; Zhu et al., 2017). TLS data was used to estimate LAD using indirect radiometric inversion (Zhao et al., 2015). TLS data was also used to visually delineate individual leaf (Béland et al., 2011), and automatically reconstruct leaf surface and normal vectors at individual tree scale (Zheng and Moskal, 2012). However, there was no leaf size constraint in the leaf reconstruction. Instead, a fixed number of 6 neighboring points was used to form each leaf surface (Zheng and Moskal, 2012). This may be problematic for upper canopy layers when point density is low, making the distance amongst the 6 points much larger than the size of an individual leaf. Recently, a rapid LAD estimation method was developed based on triangulation of TLS point clouds (Bailey and Mahaffee, 2017). This method demonstrated good accuracy for an isolated tree and a vineyard. However, the calculated LAD should be more precisely named plant angle distribution, as leaf and woody material were not differentiated.

To the best of our knowledge, the leaf angle distribution (LAD) variation has only been quantified at individual canopy level by manual measurement (Wirth et al., 2001; Holder, 2012), digital canopy photography methods (Raabe et al., 2015), or digital stereo imaging (Muller-Linow et al., 2015). All these methods are difficult to implement in natural forests. The objective of this research is therefore as follows. First, improving the LAD estimation from TLS by considering the leaf size constraint, as well as excluding mixed effects from woody material. Second, exploring whether there is LAD variation at different canopy layers in European beech (*Fagus sylvatica*) forests. Third, exploring whether there is LAD variation across beech stands at different succession status.

2. Study area and data collection

2.1. Study area, plant description and plot distribution

The study area is the Bavarian Forest National Park, located in southeastern Germany. It is a low mountain range forest ecosystem in Central Europe, with elevation ranging from 650 m to 1453 m. It is located in the temperate climate zone and is subject to maritime and continental influences (Bässler et al., 2008). Mean annual precipitation is between 830 and 2230 mm depending on altitude. Dominant tree species are Norway spruce (*Picea abies*) (67%) and European beech

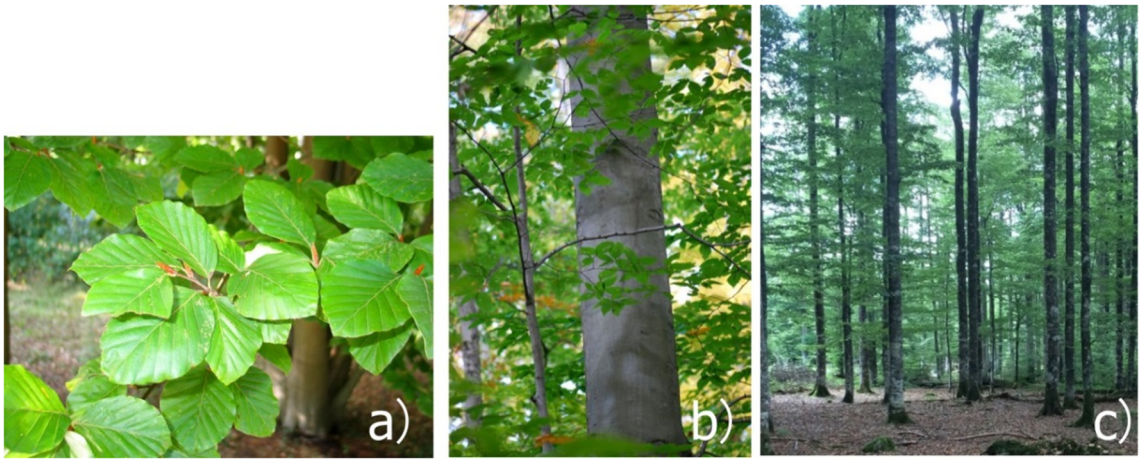

Fig. 2. European Beech (*Fagus sylvatica*) in the Bavarian Forest National Park. (a) leaves; (b) trunk and branch; (c) a mature plot.

(*Fagus sylvatica*) (24.5%) (Cailleret et al., 2014).

In this research, European beech is selected due to its broadleaf feature, as well as its wide distribution in Western and Central Europe. Beech trees normally grow to 30–35 m (up to 50 m in optimal conditions) tall. A 15-year-old sapling stands about 4 m. The bark of European beech is smooth as seen in Fig. 2(b). The leaves are elliptical without any lobes and have a short stalk, as seen in Fig. 2(a). Leaf size ranges from 25 to 40 cm^2, with 5–10 cm long and 3–7 cm broad (Barna, 2004). European beech is a highly shade-tolerant species, which can regenerate naturally in continuous cover. In Central Europe, it is the most abundant broadleaf forest tree, because of its physiological tolerance and competitiveness (Ellenberg and Leuschner, 2010).

In total, 36 European beech plots were selected as shown in Fig. 3. They covered a wide range of stand structures and were further categorized into “young, medium, mature” stands using ancillary land cover classification data (Silveyra Gonzalez et al., 2018) and canopy height information. The structural information, including the median and standard deviation of canopy height, was extracted from airborne laser scanning data in 2016. More details can be seen in Table 1 in Appendix A.

2.2. Data collection

From 17-July to 9-August in 2017, 36 beech plots were visited during leaf-on conditions. A Riegl VZ-400 TLS was used to scan each

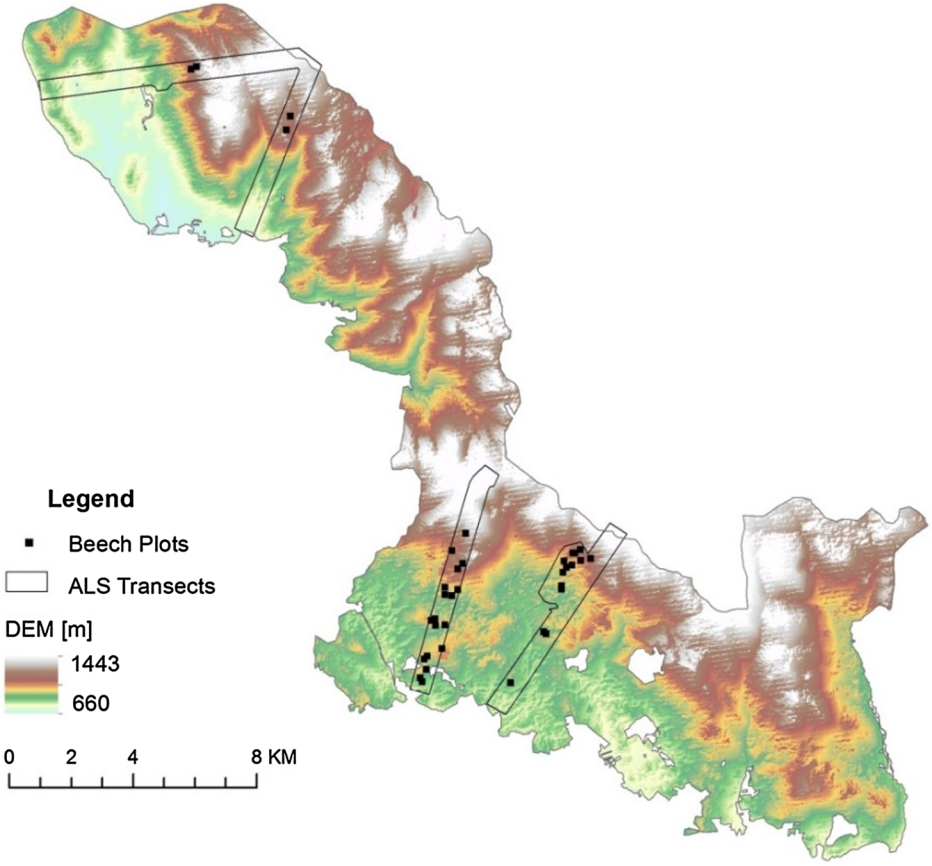

Fig. 3. The distribution of 36 European beech plots in the Bavarian Forest National Park.

plot. The scanner employs a laser (wavelength 1550 nm) with beam divergence of 0.3mrad and range accuracy of 5 mm. The footprint diameter is 0.15 cm at 5 m distance, 1.05 cm at 35 m distance. The measurement range is up to 600 m. The angular step was set to 0.04° for the fieldwork. One center and three triangular scan positions were used in each plot, to reduce occlusion and increase point density. To achieve co-registration of the four scans, 12–18 retro-reflective targets were placed as control points. In total, it took 1–2 h to finish all scanning in a plot.

In addition to TLS data, four transects in the park were also scanned by airborne laser scanning (ALS) in August 2016, seen in Fig. 3. The sensor used was Riegl LMS Q680-i, operating at a wavelength of 1550 nm, with beam divergence of 0.5mrad. The flying altitude was approximately 300 m above ground. The average point density for each flight line was 70 points/m^2. The ALS data was used to calculate basic plot structure metrics including canopy height model (CHM), the median and standard deviation of canopy height (details in Table A1 in Appendix A).

3. Method

3.1. Preprocessing

First, the four TLS scans were co-registered and merged into one for each plot, to maximize point density, using the RiScan Pro software (http://www.riegl.com). The average registration error was 3–8 mm. Then, a point cloud with a radius of 15 m was clipped. Each point consisted of multiple attributes, including the Cartesian coordinates (x, y, z), laser shot direction (azimuth and zenith angle), target distance, amplitude of the echo, GPS timestamp, target surface relative reflectance, pulse shape deviation, etc.

Filtering was conducted to remove noisy points, based on the pulse shape deviation value. Pulse shape deviation may be interpreted as a measure of the reliability of the range measurement (Pfennigbauer and Ullrich, 2010). The overall quality of the point cloud can be improved by setting up a maximum allowed deviation value. In this research, all points with deviation above 20 were eliminated. This threshold was based on suggestions from previous research (Pfennigbauer and Ullrich, 2010; Greaves et al., 2015).

After noise filtering, ground returns were identified and the local height of each point was calculated using LAStools software (Isenburg, 2012). All points below 1.5 m such as ground and grass were removed from subsequent analysis. The overview of 36 plots after preprocessing can be seen in Fig. A1 in Appendix A.

3.2. Differentiating between leaf and woody material

TLS has shown promising results in differentiating leaf and woody material (Beland et al., 2014; Ma et al., 2016; Zhu et al., 2018). In this research, the point cloud was classified into leaf or woody points, thus eliminating the effect of woody material to retrieve LAD rather than PAD.

The classification followed the method using both radiometric and geometric features (Zhu et al., 2018). The significant difference in reflectivity between leaf and woody material at the 1550 nm wavelength forms the basis to use radiometric features. The bark has high reflectance, while leaves have low reflectance due to water absorption. Geometric features of leaf and woody material are also different. Leaves have planar shape, while woody material is more likely to have linear shape. A list of selected features (seen in Table 1) was calculated for each point, for the detailed equation one can refer to (Demantke et al., 2011; Zhu et al., 2018).

After feature calculation, the Support Vector Machine (SVM) classifier was used to differentiate leaf and woody points. SVM is a supervised non-parametric statistical learning technique. It shows to achieve good results even with small training datasets in high dimensional feature space (Melgani and Bruzzone, 2004), often producing higher classification accuracy than other methods (Foody and Mathur, 2004). In this research, training samples were manually selected from one plot at different layers (top, middle and bottom layer). Then the points were labeled with a class of either “leaf” or “woody” based on visual interpretation. These training samples (357 leaf points and 359 woody points) were used to build the SVM model, and applied to all 36 plots. After initial classification, a post filtering was conducted on all detected leaf points. If the majority of the neighboring points of a leaf point are woody points, then the class label of this point was changed to ‘woody’. Classification accuracy was evaluated in all 36 plots. For each plot, the point cloud was first partitioned into 12 sector cylinders (0°, 30°,…, 360°), and sliced into 10 vertical layers (1/10, 2/10, … 1). Then a random point was selected from each of these 120 sub point clouds. To define the true class label of each test sample point, all its neighboring points within a 50 cm radius spheroid were displayed. With the help of contextual information, (i.e. the point locates in a branch or a leaf), the class label (wood or leaf) of this point could be determined through visual interpretation. The classification accuracy was then calculated.

Table 1
Radiometric and geometric features used to differentiate leaf and woody points.

Type	Feature	Description
Radiometric features	Ref	Calibrated relative reflectance
	Ref_{mean}	Mean Ref of the local points
	Ref_{std}	Standard deviation of Ref of the local points
	Dev	Pulse shape deviation
Geometric features	α_{1D}	The likelihood that the shape of the local points is linear
	α_{2D}	The likelihood that the shape of the local points is planar
	α_{3D}	The likelihood that the shape of the local points is random
	Z_{diff}	Range of maximum and minimum height value of the local points
	Z_{std}	Standard deviation of height in the local points

3.3. Reconstructing surface and calculating normal vector

After classification, individual leaf surfaces were reconstructed on the leafy point cloud through plane fitting constrained by leaf size. Let $S = p_i$ (x, y, z), i ∈ [1, N_{total}] be the point cloud of the plot in the Cartesian coordinate system, N_{total} is the number of all points. For point p_k, its neighboring points $S' = (p_1, p_2,\ldots, p_n)$ could be identified by searching all points in S that are within a distance L_{max} of point p_k. If the number of neighboring points, i.e. n, is greater than 5, these points were considered to form a leaf surface. The normal vector of S’ was calculated through principal component analysis. The normal vector direction is the same as the direction of the eigenvector with the minimum eigenvalue. If n is smaller or equal to 5, point p_k was considered as an isolated point, and eliminated from subsequent analysis. In theory, within the L_{max} radius, 3 points can form a plane. However to avoid uncertainty caused by noise points, we used 5 neighboring points (in total 6 points) to do the plane fitting. For more discussion on this, one can refer to a previous study (Hoppe et al., 1992). It should be noted that in this method, no differentiation was made between leaves having an adaxial sky facing surface or abaxial sky facing surface, thus all leaf inclination angles are positive.

The radius of this neighborhood distance L_{max}, should be constrained by the leaf size. If the value of L_{max} is very low, many points were processed as isolated points and eliminated, since their neighboring points are beyond the distance of L_{max}. However, if the value of L_{max} is very high, points from two adjacent leaves may be merged into one neighborhood S'. In a previous research, L_{max} was set to be 5 cm (Bailey and Mahaffee, 2017). In this research, after considering the leaf

size of European beech (as mentioned in Section 2.1, usually 5–10 cm long and 3–7 cm broad), L_{max} was set to be 4 cm.

3.4. Validating accuracy of the leaf angle calculation method

In order to evaluate the accuracy of the leaf angle calculation method, we generated a simulated dataset, where the location and the true angle of each leaf was known, similarly to techniques used in previous research (Zheng and Moskal, 2012; Bailey and Mahaffee, 2017; Li et al., 2018). First, the 3D models of two synthetic beech trees, one young (3 m high, 1122 leaves) and one mature (30 m high, 21,534 leaves) were constructed using the open source software Arbaro (http://arbaro.sourceforge.net/). The LiDAR simulator HELIOS (Bechtold and Höfle, 2016) was employed to 'scan' the beech tree, using the same settings as used in the fieldwork (0.3 mrad beam divergence, 0.04° angular step, 7.5 m distance away, 3 scans). For the mature tree, titled (90°) scans were used to ensure coverage on the canopy top. Leaf angles were calculated using our proposed method from the simulated TLS point cloud. The calculation accuracy was evaluated in the 'leaf-wise' way, by comparing all leaf angles estimated from the simulated TLS point cloud with true leaf angles from the 3D models. The coefficient of determination (R^2), the root mean square error (RMSE), and the normalized RMSE (nRMSE) were used to evaluate the performance of the method.

3.5. Statistical analysis

LAD was retrieved through calculating the histogram of the inclination angles of all reconstructed leaf surfaces, as the frequency distribution from 0° to 90° with 1° bin width. Four statistical parameters of the leaf angle distribution (LAD) were also calculated, including the median angle (θ_{median}), the average angle (θ_{mean}), the most frequent angle (θ_{mode}), and skewness of LAD (*skewness*). In addition, each LAD was classified into one of the six categorical (planophile, plagiophile, uniform, spherical, erectophile, extremophile) LAD functions (de Wit 1965) as detailed in Fig. 1. This was done by quantifying the similarity of plot LAD with the six pre-defined LAD functions (Pisek et al. 2013) through the following three metrics,

$$\chi_1 = \sum_{\theta=0}^{90} |f(\theta) - f_{deWit}(\theta)| \quad (1)$$

$$\chi_2 = \sqrt{\frac{\sum_{\theta=0}^{90} (f(\theta) - f_{deWit}(\theta))^2}{90}} \quad (2)$$

$$\chi_3 = \frac{|f(\theta) \cap f_{deWit}(\theta)|}{|f(\theta) \cup f_{deWit}(\theta)|} = \frac{\sum_{\theta=0}^{90} \min(f(\theta), f_{deWit}(\theta))}{\sum_{\theta=0}^{90} \max(f(\theta), f_{deWit}(\theta))} \quad (3)$$

The pre-defined LAD which had the lowest χ_1, χ_2, or highest χ_3 will be voted as similar to the plot LAD. The LAD type, which received the highest count of votes, was chosen as the classification result for the plot LAD.

In order to explore the variation of LAD on different height levels in a canopy, each plot was divided into 3 layers according to the local height of each point. Let H_{max} be the maximum canopy height. Points with greater than 80% H_{max} were treated as the top layer. Points at 80% to 20% H_{max} were regarded as the middle layer. Points below 20% H_{max} were used as the bottom layer. The above-mentioned analyses were conducted on each layer of each plot.

In order to explore the variation of LAD across stands, the above-mentioned analyses were conducted for each plot. The correlation coefficient was calculated between θ_{mean} and the plot median canopy

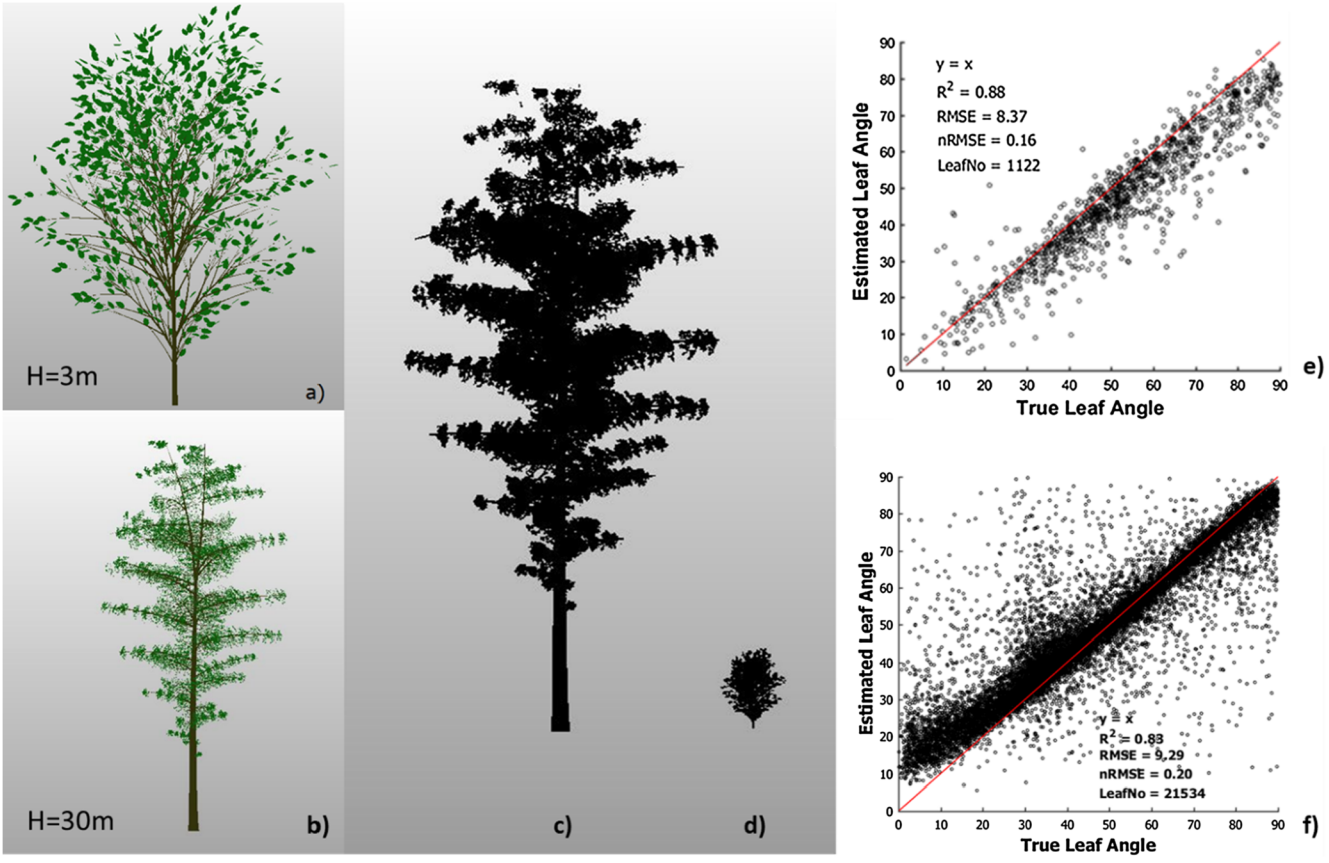

Fig. 4. Results of the leaf angle calculation accuracy using simulated dataset: (a) and (b) the 3D models of two synthetic beech trees; (c) and (d) the simulated TLS point clouds of the beech trees; (e) and (f) true leaf angles and leaf angles estimated using the proposed method.

height, to explore the relationship between plot LAD and plot successional status. A positive close to 1 correlation coefficient would suggest a strong positive correlation between the θ_{mean} and the stand successional status.

4. Results

4.1. Accuracy of leaf angle calculation

From the simulated dataset, we compared the TLS estimated leaf angles with true leaf angles directly read from the synthetic beech tree model. Through this, we can evaluate the accuracy of our proposed method. From the results in Fig. 4, for the synthetic young beech tree (3 m high, with 1122 leaves), the proposed method works very well (R^2 = 0.88, RMSE = 8.37°, nRMSE = 0.16). For the synthetic mature beech tree (30 m high, with 21,534 leaves), although there are some leaves with larger estimation errors for leaf angle, the overall accuracy remains high (R^2 = 0.83, RMSE = 9.29°, nRMSE = 0.20).

4.2. Results of differentiating leaf and woody materials

In this study, the overall classification accuracy when differentiating leaf and woody materials is 87.59% across 36 beech plots, with the accuracy of each plot ranging from 78.26% to 94.32% (details in Table A1 in Appendix A). An example of the classification result is displayed in Fig. 5. Large tree trunks and smaller branches could be accurately detected. At 8 m level, most leaves were covered by dense points and were accurately detected, shown in Fig. 5(c). However, small twigs were often misclassified as leaves. Similar results occurred at the 16 m level in Fig. 5(d). Although the point density was not as high as at lower height levels, tree trunks, branches, and leaves could still be differentiated. But fine twigs were again misclassified as leaves.

4.3. Variation of leaf angle distribution on different canopy layers

An example of the 3D distribution of leaf inclination angle in a mature plot is shown in Fig. 6. In the top layer, many leaves are displayed as red and yellow colors (50–80°), indicating a more vertical growing direction. But in the middle layer and bottom layer, most leaves display blue or cyan colors (10–40°), indicating a more horizontal and lateral growing direction.

From statistical parameters and leaf angle distribution (LAD) classifications in Fig. 6(g), LAD in the top layer is most similar to the uniform distribution, with largest θ_{median}, θ_{mean}, θ_{mode}, and lowest skewness. But LAD the middle and bottom layers is most similar to the planophile distribution. The θ_{median}, θ_{mean} and θ_{mode} decrease, while skewness rises. In general, from the top to bottom layer, the frequency of vertical leaves decreases, while the frequency of more horizontal (oblique) leaves increases.

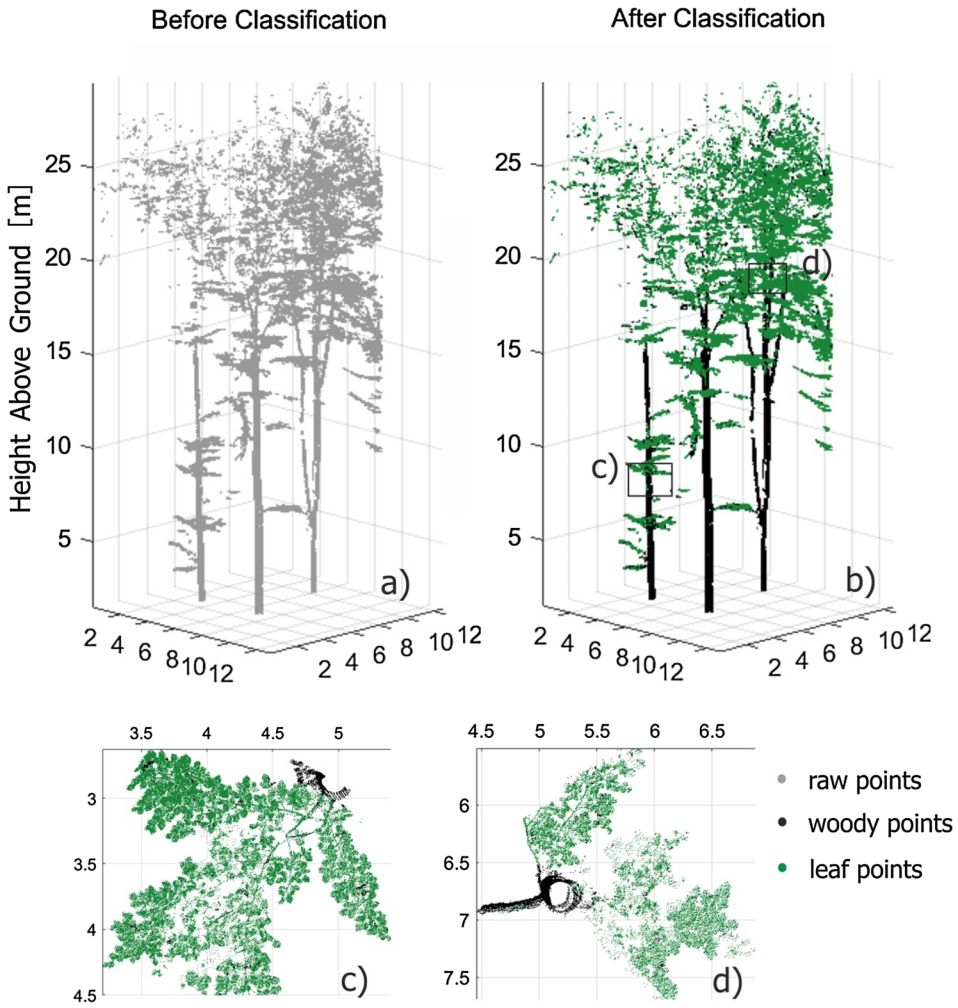

Fig. 5. Results of differentiating leaf and woody points in part of a mature beech plot B32: (a) before and (b) after classification; detailed results at (c) 8 m and (d) 16 m above ground.

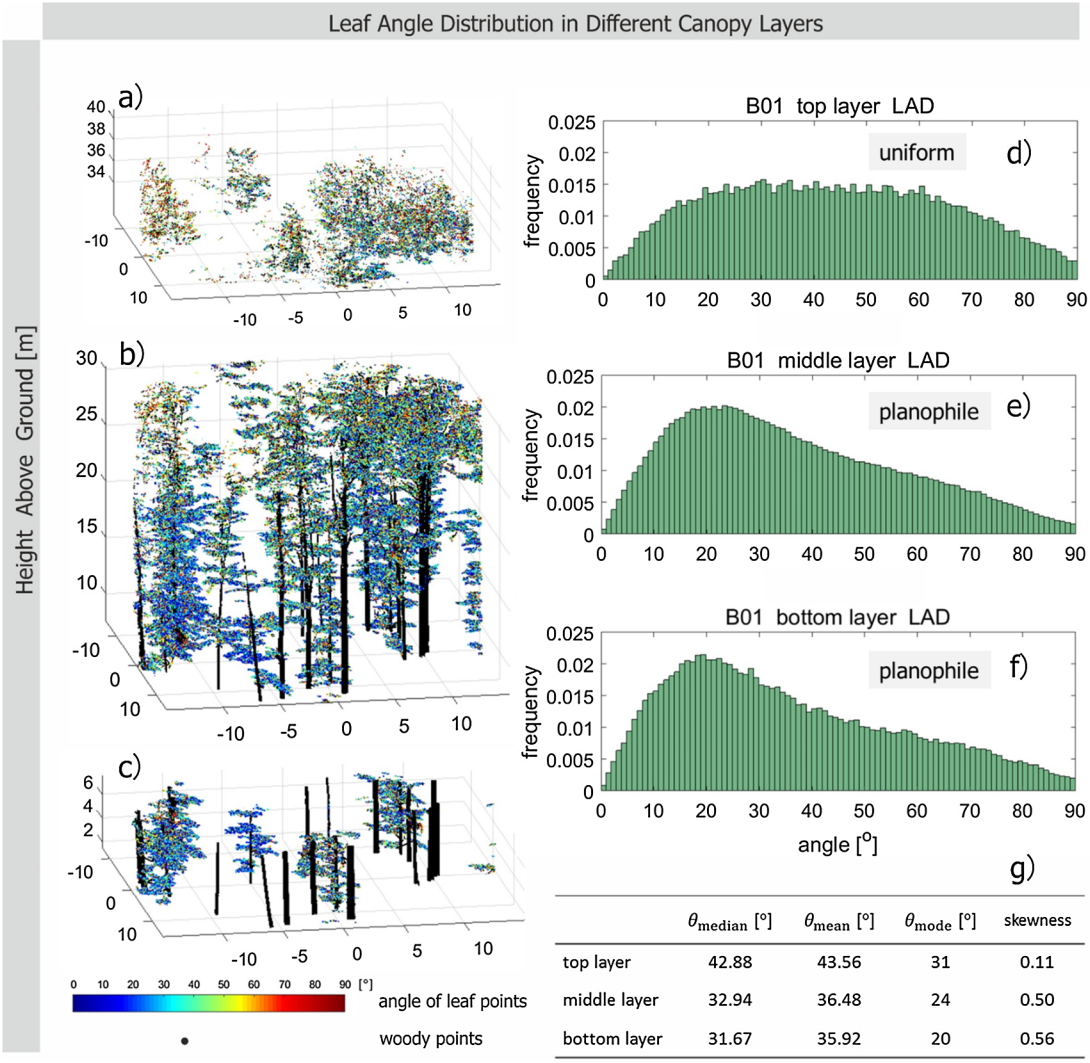

	θ_{median} [°]	θ_{mean} [°]	θ_{mode} [°]	skewness
top layer	42.88	43.56	31	0.11
middle layer	32.94	36.48	24	0.50
bottom layer	31.67	35.92	20	0.56

Fig. 6. Leaf angle distribution (LAD) at different canopy layers in the mature beech plot B01. (a)–(c) are the 3D distribution of leaf angles; (d)–(f) are the LAD histograms; (g) summary of statistics.

4.4. Variation of leaf angle distribution across stands at different succession status

The 3D distribution of leaf inclination angles in three different stands can be seen in Fig. 7. In a young plot B27 with beech regeneration, stem density is low. Beech canopies have a spheroid rather than cylinder shape, as seen in Fig. 7(d), with leaves orientated in various directions. In a medium plot B10, stem density becomes much higher. Leaves grow in various directions in the top layer, but grow more horizontally in the middle layer. In a mature plot B31, the vertical difference of LAD becomes more pronounced.

Statistical parameters demonstrate moderate variation of LAD across these three stands (Fig. 8). From young to mature stands, the θ_{mean} decreases about 8°, while θ_{mode} decreases 22° (see Table 2). The LAD of the young plot B27 and medium plot B10 is most similar to the uniform distribution, but LAD of the mature plot B31 is most similar to the planophile distribution, with a highly positive *skewness* of 0.42.

The LAD variation across all 36 stands is detailed in Fig. 9. The relationship between LAD and stand successional status was explored by inspecting θ_{mean} and *skewness* with the median canopy height in the plot (CHM_{median}). Interestingly, plot θ_{mean} is strongly negatively related to CHM_{median} ($r = -0.70$, $p < 0.001$), while skewness of LAD is moderately positively related to CHM_{median} ($r = 0.64$, $p < 0.001$). In young and medium plots ($CHM_{median} \in [4, 20]$ m), LAD is most similar to the uniform distribution with low skewness. However in mature plots ($CHM_{median} > 20$ m), LAD is most similar to the planophile distribution with high skewness. Among all 36 plots, the difference between minimum and maximum θ_{mean} is moderate (10°, from 36.91° to 46.14°). It is also worth noted that the LAD in all plots are quite different from the spherical distribution.

The LAD variation at different canopy layers in all 36 plots is shown in Fig. 10. From paired sample *t* test, for all plots, the LAD in the top layer has the highest θ_{mean} ($p < 0.001$), the highest θ_{mode} ($p < 0.001$) and the lowest *skewness* ($p < 0.001$). There is no statistical significant difference in θ_{mean} ($p = 0.586$), θ_{mode} ($p = 0.704$) and *skewness* ($p = 0.690$) of the middle layer and bottom layer. This indicates that beech leaves in the top layer grow more vertically.

From Fig. 10, in young and medium plots when CHM_{median} is below 20 m, the top layer has a spherical or plagiophile LAD ($\theta_{mean} \in [47°, 55°]$, $skewness \in [-0.4, 0]$). In contrast, the middle and bottom layer have an uniform LAD ($\theta_{mean} \in [41°, 47°]$, $skewness \in [0,0.4]$). In most mature plots, when CHM_{median} is above 20 m, the top layer becomes uniform or plagiophile LAD ($\theta_{mean} \in [43°, 51°]$, $skewness \in [-0.2, 0.1]$). The middle and bottom layer have a planophile LAD ($\theta_{mean} \in [33°, 45°]$, $skewness \in [0.1, 0.8]$).

Additional statistics can be seen in Table A1 in Appendix A. Out of all 108 layers from 36 plots, there is a large variation of θ_{mean} (from 33.64° to 52.97°), while the variation of θ_{mode} is even higher (from 14°

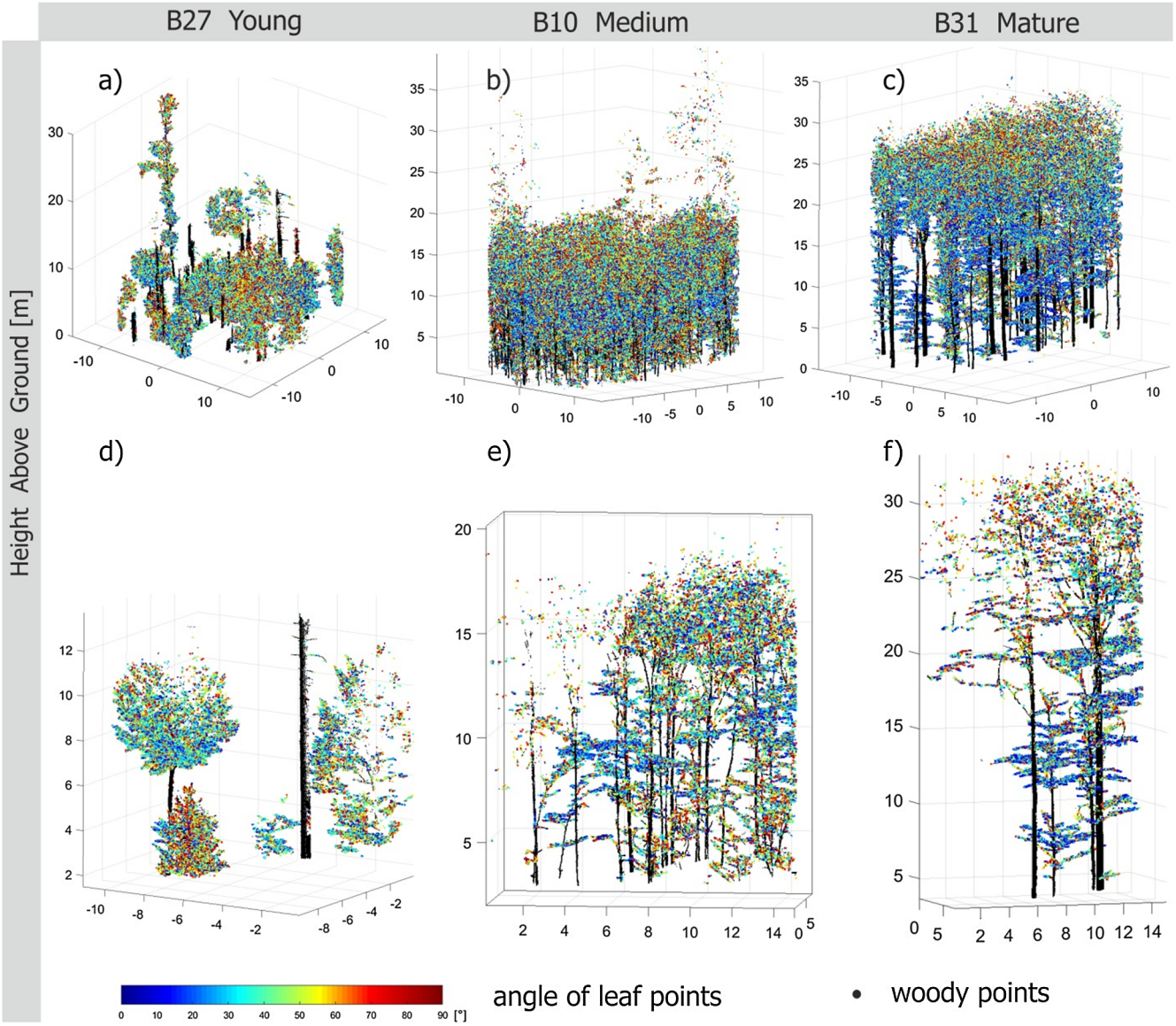

Fig. 7. Leaf angle distribution (LAD) on plots of different successional status. The 3D distribution of leaf angles in (a) a young plot B27; (b) a medium plot B10; (c) a mature plot B31; (d) part of B27; (e) part of B10; (f) part of B31.

to 64°). 20 of the 36 plots have an inner plot vertical θ_{mean} difference of more than 15% (maximum difference = 28.18%, from 33.64° to 46.84°). 23 plots have an inner plot vertical θ_{mode} difference of more than 40% (maximum difference = 69.57%, from 14° to 46°). This demonstrates inner-plot vertical variation of LAD is even more severe than inter-plot variation of LAD.

5. Discussion

5.1. Variation of leaf angle distribution in European beech forests

In this research, moderate leaf angle distribution (LAD) variation was found across European beech plots in different succession status, and they are all quite different from the spherical distribution. This led us to question the widespread simplification of LAD as the spherical distribution (Richardson et al., 2009; Tang et al., 2012) in previous research. In mature stands, we found planophile LAD, which is consistent with previous research where the average leaf inclination angle of beech forests is reported to be around 21.7° (Wagner and Hagemeier, 2006), 31° (Chianucci et al., 2015) and 18.08° (Chianucci et al., 2018). It is also consistent with the planophile LAD suggestion for temperate broadleaf forests (Pisek et al., 2013). However, in young and medium stands, LAD is most similar to the uniform rather than planophile distribution.

An important new discovery from this research is that there is a strong negative correlation ($r = -0.70$, $p < 0.001$) between the median canopy height of a plot and the average leaf inclination angle θ_{mean} of the plot, for natural European beech forests. From young to the taller mature stands, LAD changed from symmetric uniform or plagiophile distribution to a skewed planophile distribution. This implies that in situations where canopy height or stand age data is available, it is possible to estimate plot-specific LAD. This offers the potential to upscale this study and map LAD at airborne or satellite level using airborne or satellite LiDAR data.

There is even larger variation of LAD on different canopy layers ($\theta_{mean} \in [33.64°$ to $52.97°]$, $\theta_{mode} \in [14°$ to $64°]$) quantified by TLS. A general trend is that leaves grow more vertically in the top canopy layer, and grow more horizontally in the middle and bottom layers. This is consistent with previous studies, where leaves were found more horizontal in understory beech saplings (Planchais and Pontailler, 1999; Balandier et al., 2007; Chianucci et al., 2014) or shaded beech saplings (Delagrange et al., 2006). Based on the results in Sections 4.3

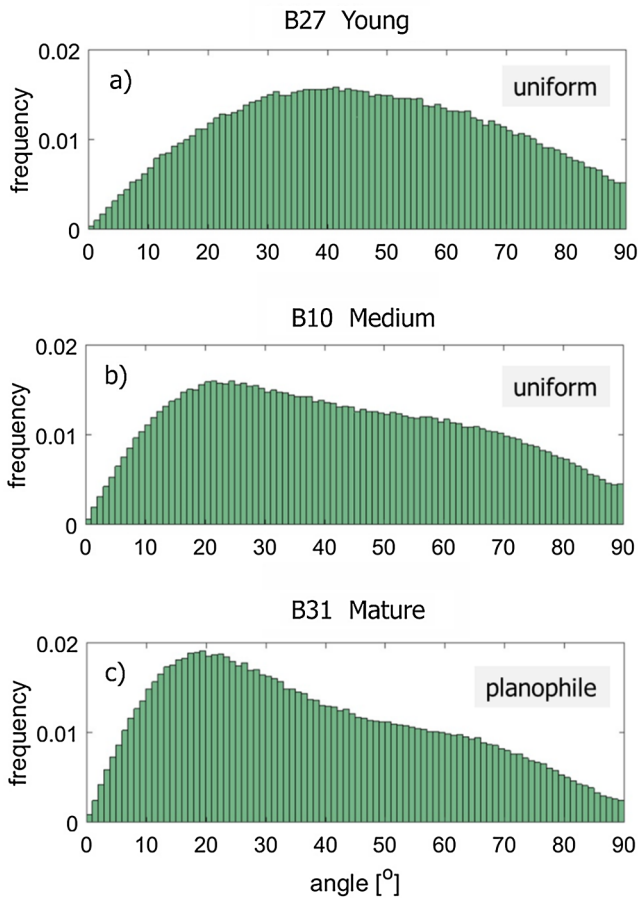

Fig. 8. Leaf Angle Distribution (LAD) on plots of different successional status: (a) a young plot B27; (b) a medium plot B10; (c) a mature plot B31.

Table 2
Summary of statistics of leaf angle distribution (LAD) across three different stands.

Plot name	Successional status	θ_{median} [°]	θ_{mean} [°]	θ_{mode} [°]	skewness
B27	Young	45.43	46.14	42	0.07
B10	Medium	40.24	42.28	25	0.23
B31	Mature	34.38	37.98	20	0.42

θ_{median}: median leaf angle.
θ_{mean}: average leaf angle.
θ_{mode}: most frequent leaf angle.
skewness: skewness of LAD.

and 4.4, we recommend when in-situ LAD data are not available, the choice of predefined functions for LAD approximation could follow instructions in Table 3.

There may be many reasons for such variation of LAD in European beech forests. LAD can be viewed as a morphological or structural trait of plants. Plant traits can reflect the outcome of evolutionary and community assembly processes responding to abiotic and biotic environmental constraints (Valladares et al., 2007; Kattge et al., 2011). The vertical variation of LAD in European beech plots can be interpreted as a result of plant adaptation to different light availability at different canopy layers. On the one hand, leaves in the top layer have a higher chance of direct sun, so steeper leaf angles can help reduce exposure to excess radiation and consequent water stress during the middle of the day (Falster and Westoby, 2003), as well as allowing more light to reach the lower canopy. On the other hand, leaves in the middle and bottom layer are more likely to be shaded leaves, with a flatter inclination enhancing light interception under low light levels (Niinemets, 2010). These mid to low canopy position leaves are also less susceptible to high evapotranspiration due to canopy shading (Ryu et al., 2011). The more horizontal inclination may also be a strategy to eliminate competition from other species (Niinemets, 2010). A similar trend of more planophile LAD in lower canopy was also found in an oak forest in the UK (Kull et al., 1999), a mixed deciduous forest in the US (Hutchison et al., 1986) and a mature tropical moist forest in Republic of Panama (Wirth et al., 2001), where researchers used only one stand and estimated LAD manually. The negative correlation of LAD with the median canopy height of the plot, may be due to the increasing percentage of leaves under low light conditions inside the canopy relative to the crown periphery. This led to an increasing percentage of leaves with low leaf inclination angles, thus leading to a decrease in θ_{mean}.

5.2. Factors affecting LAD retrieval from TLS

Compared to manual measurement and digital canopy photography method, TLS has the advantage of rapid data acquisition of large area, dense sampling, efficient automatic processing and less human intervention (e.g., no need to identify each leaf visually), let alone its advantage to acquire millimeter level precise geometrical information. Although this study was conducted in European beech forests, the TLS method can be transferred to many other broadleaf species, most suitable for flat leaves. It may also be used to large non-flat leaf like corn, where individual leaf can be regarded consisting of several flat patches. In the following, we will discuss some aspects, which should be considered when using TLS to quantify LAD.

5.2.1. TLS data collection and preprocessing

High quality point cloud data are prerequisite for LAD retrieval from TLS. A small beam divergence, small angular step, and close range is necessary for plants with small leaves. Otherwise the TLS footprint may be larger than individual leaf, making leaf surface reconstruction impossible. The optimal settings can be calculated from the parameters of the TLS sensor and plant leaf size. For more information, one can refer to a previous research (Wilkes et al., 2017). A multiple scan position design and a small angular step are suggested to increase point density. Accurate co-registration among multiple scans ensures utilization of all scan points. While a bad co-registration and misalignment may lead to many isolated points in the leaf surface reconstruction step or create spurious objects. In addition, raw height was used in this research instead of local height, since LAD estimation involves 3D structure and topology of neighboring points. Topographic normalization will create distortion of the point cloud (Liu et al., 2017).

5.2.2. Extraction of leaf points

The classification of leaf versus woody points was very accurate in general. The main errors appear to be caused by fine scale twigs, which were wrongly classified as leaf points. This may result from high uncertainty in twig point reflectance due to “partial hits”. Because twigs are very narrow, there is a higher possibility for a laser beam to partially hit the twig and only a fraction of the laser pulse is returned (Eitel et al., 2010). In this condition, the ‘calibrated relative reflectance’ measured by Riegl VZ-400 is not valid, since the partial illumination of a bright target can yield the same measurement as a more complete illumination of a darker target (Beland et al., 2014). As a result, the reflectance of twigs was lower than other woody points, causing incorrect classification as leaves.

5.2.3. Point density effect

A potential source of uncertainty in leaf angle distribution (LAD) is the point density effect. In TLS, the spherical scanning geometry leads to a higher point density of near-range objects than far-range objects (Jupp et al., 2009; Zhao et al., 2015). Point density was shown to influence the retrieval accuracy of canopy height, canopy cover, and biomass (Jakubowski et al., 2013; Wilkes et al., 2015; Garcia et al.,

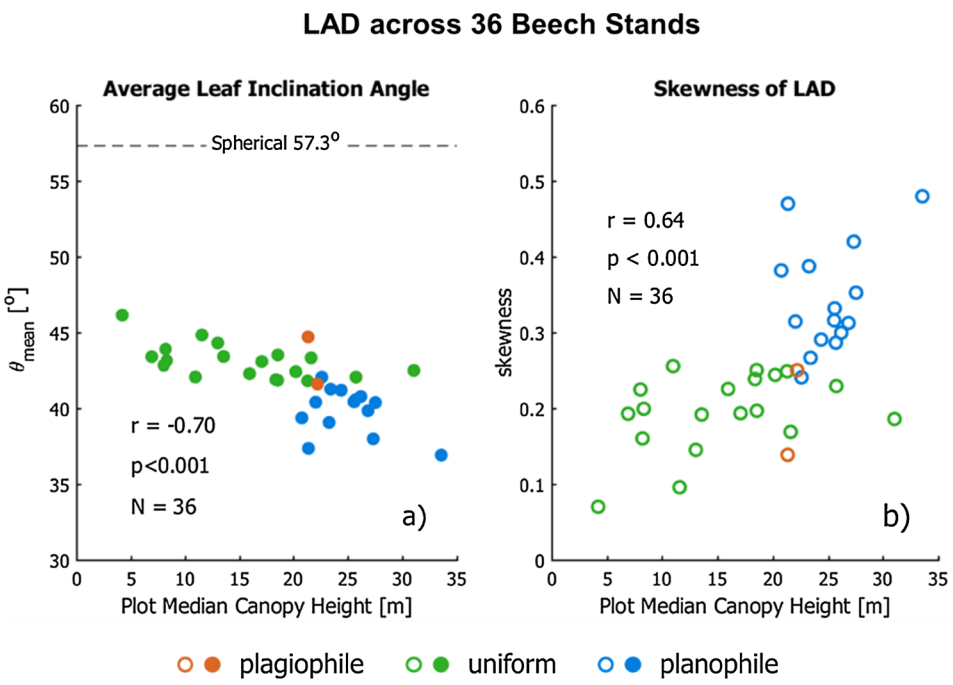

Fig. 9. The correlation between plot median canopy height and plot (a) average leaf inclination angle and (b) skewness of leaf angle distribution (LAD) across all 36 European beech plots.

2017). Therefore, the point density effect on leaf angle calculation was analyzed.

We used the mean nearest neighbor points distance (MNNPD) (Wilkes et al., 2017) to quantify point density. Sparse point clouds have high MNNPD while dense point clouds have high MNNPD. In all 36 beech plots, with increasing height above ground, MNNPD increases from 0.24 cm to 2.86 cm shown in Fig. 11(a). To mimic this point density change, the simulated TLS point cloud of the synthetic young beech tree was thinned to different levels. First, we randomly selected points from the raw TLS data at different percentages, from 5% to 20% at a step of 1%, from 20% to 100% at a step of 5%. In total 32 point clouds were generated. Second, the leaf angle calculation and accuracy evaluation was implemented for each point cloud. From the results (Fig. 11b), leaf angle estimation became less accurate (R^2: 0.88 - > 0.52, RMSE: 8.37° - > 12.39°) with a decreasing point density (or increasing MNNPD). It can be concluded that at a height of 0–20 m above ground, the leaf angle estimation is very accurate (MNNPD < 1.4 cm, R^2 > 0.75, RMSE < 9.5°). From 20 to 30 m, leaf angle estimation is moderately accurate (MNNPD < 2.4 cm, R^2 > 0.6, RMSE < 11.5°). Above 30 m, leaf angle estimation is roughly accurate (MNNPD < 3 cm, R^2 > 0.5, RMSE < 13°). In future studies, for more accurate leaf angle measurements of tree tops (above 30 m), it is recommended to combine with TLS scans below canopy with an UAV LiDAR scan above canopy.

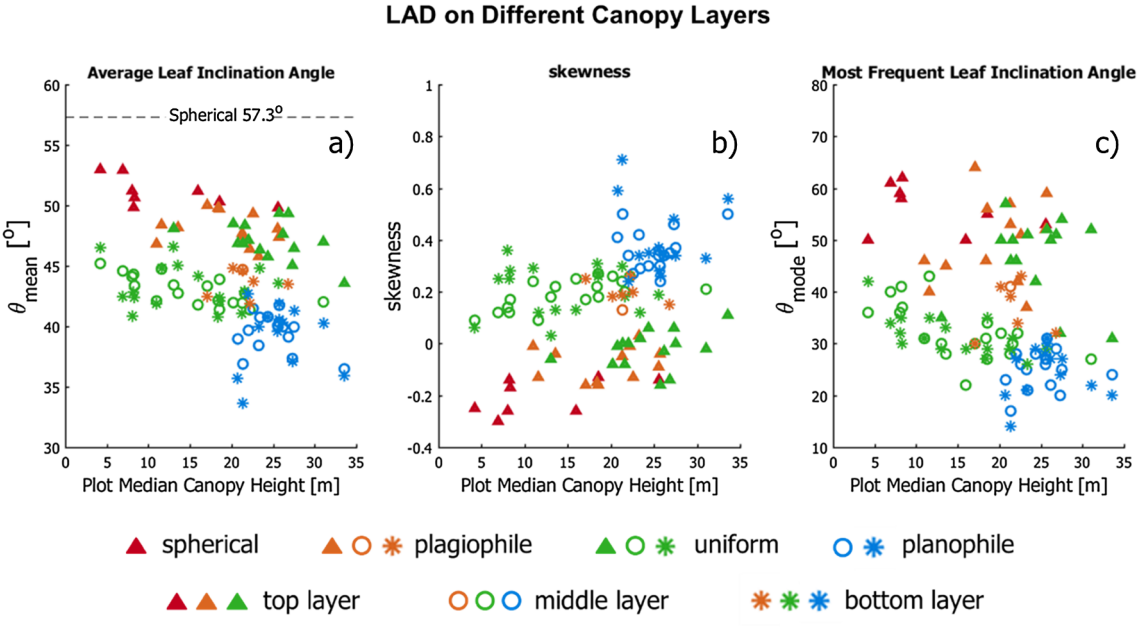

Fig. 10. Leaf angle distribution (LAD) variation at different canopy layers and across different stands, (a) average leaf inclination angle; (b) most frequent leaf inclination angle; (c) skewness of LAD.

Table 3
Suggested choice of predefined functions for leaf angle distribution (LAD) approximation in European Beech stands.

		Previous	From this research	
			Young or medium plots (< 20 m)	Mature plots (> 20 m)
Multi-layer	Top	\	Spherical	Uniform
	Middle		Uniform	Planophile
	Bottom		Uniform	Planophile
Plot averaged		Spherical	Uniform	Planophile
			Or estimate from canopy height data	

5.2.4. Evaluation of leaf angle distribution

Evaluating the LAD accuracy is extremely difficult due to challenges in manually measuring true leaf angle. Especially in natural forests, it is virtually impossible to find nearby tall buildings or observation towers as used in previous studies (Raabe et al., 2015), to remotely observe and measure leaf angles. Although it is possible to use ladders or tree climbing to reach higher levels in a tree, the movement usually disturbs the canopy and changes leaf angles (Zheng and Moskal, 2012). Therefore, in this study, the accuracy of the proposed method was evaluated using a simulated dataset. The results demonstrated that the leaf angle calculation were very accurate in general. It should be highlighted that compared to terrestrial LiDAR data scanned from real forests, the simulation data have perfect registration, less noisy points, and no errors for woody material classification (since the material type is known from the beech tree model). Future studies may investigate the effect of these factors on LAD measurement. In addition, future work can improve the validation set up using realistic synthetic stands instead of individual synthetic tree. Such stands may be created following two steps. First, the woody architecture of trees can be extracted from terrestrial LiDAR point clouds of real forests (Raumonen et al., 2013). Second, the woody materials are inserted with predefined synthetic leaves (Akerblom et al., 2018).

5.3. Management implications

The findings in this research may improve the accuracy in LAI mapping. Airborne and spaceborne LiDAR has been increasingly used to map LAI (Korhonen et al., 2011; Stark et al., 2015; Tang and Dubayah, 2017). In these studies, gap fraction was first estimated by laser pulse penetration. Then LAI could be estimated based on the Possion model using,

$$P(\theta) = e^{-G(\theta)\lambda(\theta)L/\cos(\theta)} \quad (4)$$

where θ is the direction of incoming radiation, $P(\theta)$ is the gap fraction in direction θ, L is the leaf area index, $\lambda(\theta)$ is the clumping index in direction θ, $G(\theta)$ is the leaf projection function determined by LAD. However in this method, an accurate estimate of $G(\theta)$ is necessary for accurate LAI. The spherical distribution was preferred in most cases because the $G(\theta)$ can be approximated as 0.5 in any direction (see Fig. 12). But unfortunately airborne LiDAR usually operates at small scan angles from 0° to 30° (Liu et al., 2018). At this range, there is large difference among $G(\theta)$ of different LAD as shown in Fig. 12**.** If stand specific LAD can be quantified, there is potential to increase LAI mapping accuracy.

In addition, the vertical LAD variation at different canopy layers, demonstrates the necessity for multi-layer radiative transfer modelling (Kuusk, 2001; Yang et al., 2017), even for the same species. The method used in this research, could also be utilized to study plant function, forest ecology and evolution. For example, leaf inclination may change due to water stress (Biskup et al., 2007), leaf expansion and senescence. TLS could be used to acquire measurements during the live cycle of leaves under varying microclimatic conditions. The vertical variation of LAD in European beech stands as found in this research, are consistent with the discovery that late-successional stands dominated by shade tolerant species often have a more horizontal leaf inclination angles (McMillen and McClendon, 1979; Pearcy et al., 2004; Niinemets, 2010). Further research could use TLS to acquire measurements in different forest types, to explore the relationship between geography and plant structural traits.

6. Summary and conclusion

In this study, the variation of leaf angle distribution (LAD) in European beech (*Fagus sylvatica*) forests was examined using terrestrial laser scanning (TLS). A total of 36 plots ranging from young, medium to mature successional status were studied. Leaf and woody materials were differentiated based on a combination of radiometric and geometric features. Leaf surface was reconstructed and leaf inclination was subsequently calculated. From the statistical results, we conclude:

- TLS proves to be an effective tool to quantify LAD variation due to its capability to acquire massive data rapidly, differentiate leaf and woody materials, and provide precise 3D information.
- There is moderate variation of LAD across beech plots at different successional status. Instead of a spherical LAD assumption, it is more valid to assume a uniform LAD for young and medium stands, a planophile LAD for mature stands.

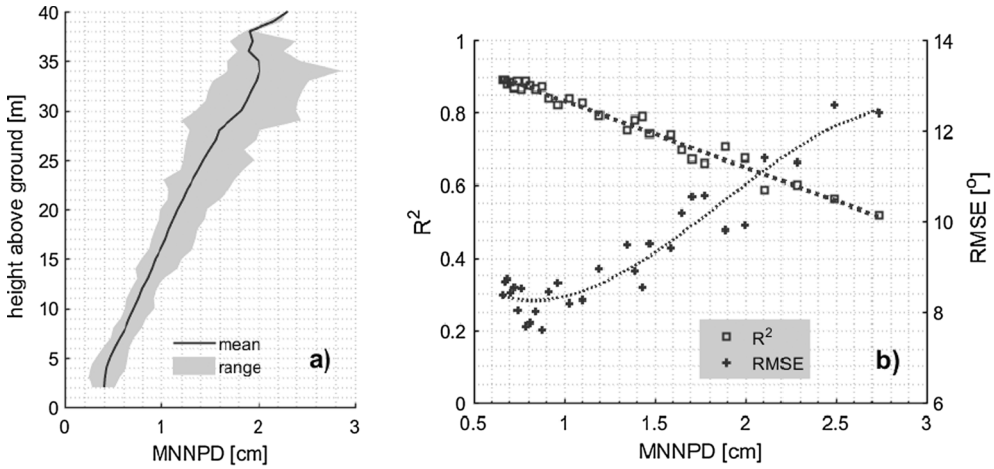

Fig. 11. (a) The decreasing point density with height above ground in all 36 beech plots (point density was quantified by mean nearest neighbor points distance (MNNPD); (b) leaf angle estimation accuracy decreases with decreasing point density from the simulated point clouds.

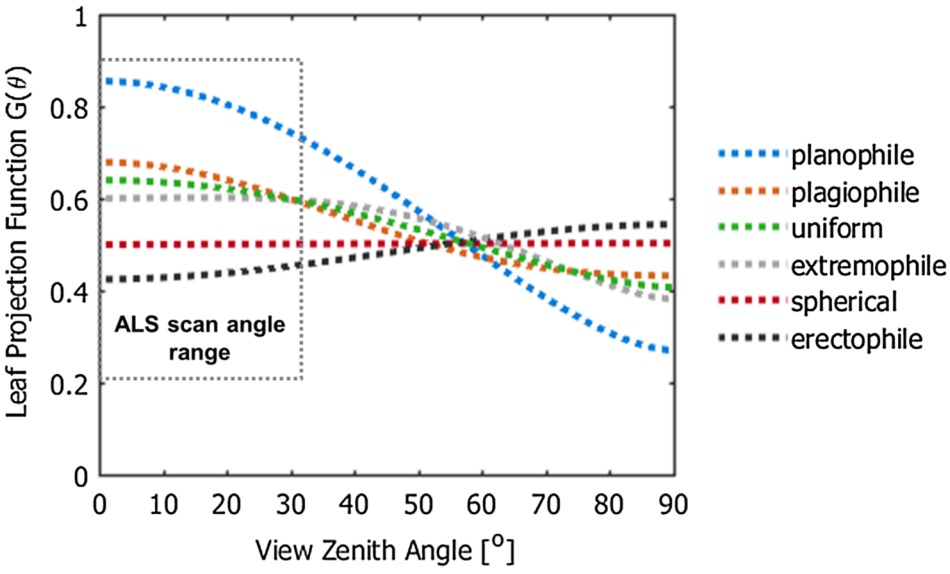

Fig. 12. Value of leaf projection function $G(\theta)$ under 6 predefined leaf angle distribution (LAD) assumptions and commonly used airborne LiDAR (ALS) scan angle range.

- There is large variation of LAD on different canopy layers. Beech leaves grow more vertically in the top layer, but more obliquely or horizontally in the middle and bottom layer.
- A strong negative correlation exists between the plot average leaf angle and the plot median canopy height. This offers the potential to estimate plot specific LAD from canopy height data in European Beech forests.
- Large variation of LAD should be accounted for better LAI mapping and canopy photosynthesis modelling.

Acknowledgments

This work was supported by the Chinese Scholarship Council under Grant 201406010295 and was co-funded by the ITC Research Fund. The authors acknowledge the support of the "Data Pool Forestry" data-sharing initiative of the Bavarian Forest National Park.

Appendix A. Supplementary material

Supplementary data to this article can be found online at https://doi.org/10.1016/j.isprsjprs.2019.01.005.

References

Akerblom, M., Raumonen, P., Casella, E., Disney, M.I., Danson, F.M., Gaulton, R., Schofield, L.A., Kaasalainen, M., 2018. Non-intersecting leaf insertion algorithm for tree structure models. Interface Focus 8.

Bailey, B.N., Mahaffee, W.F., 2017. Rapid measurement of the three-dimensional distribution of leaf orientation and the leaf angle probability density function using terrestrial LiDAR scanning. Remote Sens. Environ. 194, 63–76.

Balandier, P., Sinoquet, H., Frak, E., Giuliani, R., Vandame, M., Descamps, S., Coll, L., Adam, B., Prevosto, B., Curt, T., 2007. Six-year time course of light-use efficiency, carbon gain and growth of beech saplings (*Fagus sylvatica*) planted under a Scots pine (*Pinus sylvestris*) shelterwood. Tree Physiol. 27, 1073–1082.

Barna, M., 2004. Adaptation of European beech (*Fagus sylvatica* L.) to different ecological conditions: leaf size variation. Polish J. Ecol. 52, 35–45.

Bässler, C., Förster, B., Moning, C., Müller, J., 2008. The BIOKLIM-Project: biodiversity research between climate change and wilding in a temperate montane forest—the conceptual framework. Waldökologie, Landschaftsforschung und Naturschutz 7, 21–33.

Bechtold, S., Höfle, B., 2016. Helios: a multi-purpose lidar simulation framework for research, planning and training of laser scanning operations with airborne, ground-based mobile and stationary platforms. ISPRS Annals of Photogrammetry, Remote Sensing & Spatial Information Sciences, 3.

Beland, M., Baldocchi, D.D., Widlowski, J.L., Fournier, R.A., Verstraete, M.M., 2014. On seeing the wood from the leaves and the role of voxel size in determining leaf area distribution of forests with terrestrial LiDAR. Agric. For. Meteorol. 184, 82–97.

Béland, M., Widlowski, J.-L., Fournier, R.A., Côté, J.-F., Verstraete, M.M., 2011. Estimating leaf area distribution in savanna trees from terrestrial LiDAR measurements. Agric. For. Meteorol. 151, 1252–1266.

Biskup, B., Scharr, H., Schurr, U., Rascher, U., 2007. A stereo imaging system for measuring structural parameters of plant canopies. Plant Cell Environ. 30, 1299–1308.

Cailleret, M., Heurich, M., Bugmann, H., 2014. Reduction in browsing intensity may not compensate climate change effects on tree species composition in the Bavarian Forest National Park. For. Ecol. Manage. 328, 179–192.

Calders, K., Newnham, G., Burt, A., Murphy, S., Raumonen, P., Herold, M., Culvenor, D., Avitabile, V., Disney, M., Armston, J., Kaasalainen, M., 2015. Nondestructive estimates of above-ground biomass using terrestrial laser scanning. Methods Ecol. Evol. 6, 198–208.

Chen, J., Black, T., Adams, R., 1991. Evaluation of hemispherical photography for determining plant area index and geometry of a forest stand. Agric. For. Meteorol. 56, 129–143.

Chianucci, F., Cutini, A., Corona, P., Puletti, N., 2014. Estimation of leaf area index in understory deciduous trees using digital photography. Agric. For. Meteorol. 198, 259–264.

Chianucci, F., Macfarlane, C., Pisek, J., Cutini, A., Casa, R., 2015. Estimation of foliage clumping from the LAI-2000 Plant Canopy Analyzer: effect of view caps. Trees 29, 355–366.

Chianucci, F., Pisek, J., Raabe, K., Marchino, L., Ferrara, C., Corona, P., 2018. A dataset of leaf inclination angles for temperate and boreal broadleaf woody species. Ann. For. Sci. 75.

Coops, N.C., Hilker, T., Wulder, M.A., St-Onge, B., Newnham, G., Siggins, A., Trofymow, J.T., 2007. Estimating canopy structure of Douglas-fir forest stands from discrete-return LiDAR. Trees 21, 295–310.

de Wit, C.T., 1965. Photosynthesis of leaf canopies. In: Pudoc.

Delagrange, S., Montpied, P., Dreyer, E., Messier, C., Sinoquet, H., 2006. Does shade improve light interception efficiency? A comparison among seedlings from shade-tolerant and -intolerant temperate deciduous tree species. New Phytologist 172, 293–304.

Demantke, J., Mallet, C., David, N., Vallet, B., 2011. Dimensionality based scale selection in 3D lidar point clouds. Int. Arch. Photogram. Remote Sens. Spatial Inform. Sci. 38, W12.

Eitel, J.U., Vierling, L.A., Long, D.S., 2010. Simultaneous measurements of plant structure and chlorophyll content in broadleaf saplings with a terrestrial laser scanner. Remote Sens. Environ. 114, 2229–2237.

Ellenberg, H., Leuschner, C., 2010. Vegetation Mitteleuropas mit den Alpen: in ökologischer, dynamischer und historischer Sicht. Utb.

Falster, D.S., Westoby, M., 2003. Leaf size and angle vary widely across species: what consequences for light interception? New Phytologist 158, 509–525.

Foody, G.M., Mathur, A., 2004. A relative evaluation of multiclass image classification by support vector machines. IEEE Trans. Geosci. Remote Sens. 42, 1335–1343.

Garcia, M., Saatchi, S., Ferraz, A., Silva, C.A., Ustin, S., Koltunov, A., Balzter, H., 2017. Impact of data model and point density on aboveground forest biomass estimation from airborne LiDAR. Carbon Balance Manage. 12, 4.

Greaves, H.E., Vierling, L.A., Eitel, J.U.H., Boelman, N.T., Magney, T.S., Prager, C.M., Griffin, K.L., 2015. Estimating aboveground biomass and leaf area of low-stature Arctic shrubs with terrestrial LiDAR. Remote Sens. Environ. 164, 26–35.

Hancock, S., Essery, R., Reid, T., Carle, J., Baxter, R., Rutter, N., Huntley, B., 2014. Characterising forest gap fraction with terrestrial lidar and photography: an examination of relative limitations. Agric. For. Meteorol. 189, 105–114.

Holder, C.D., 2012. The relationship between leaf hydrophobicity, water droplet retention, and leaf angle of common species in a semi-arid region of the western United States. Agric. For. Meteorol. 152, 11–16.

Hoppe, H., DeRose, T., Duchamp, T., McDonald, J., Stuetzle, W., 1992. Surface reconstruction from unorganized points. ACM.

Hosoi, F., Omasa, K., 2009. Detecting seasonal change of broad-leaved woody canopy leaf

area density profile using 3D portable LIDAR imaging. Funct. Plant Biol. 36, 998–1005.
Hutchison, B., Matt, D., McMillen, R., Gross, L., Tajchman, S.J., Norman, J., 1986. The architecture of a deciduous forest canopy in eastern Tennessee, USA. J. Ecol. 635–646.
Isenburg, M., 2012. LAStools-efficient tools for LiDAR processing. Available at: < http://www.cs.unc.edu/~isenburg/lastools/ > [Accessed October 9, 2012].
Ivanov, N., Boissard, P., Chapron, M., Andrieu, B., 1995. Computer stereo plotting for 3-D reconstruction of a maize canopy. Agric. For. Meteorol. 75, 85–102.
Jakubowski, M.K., Guo, Q.H., Kelly, M., 2013. Tradeoffs between lidar pulse density and forest measurement accuracy. Remote Sens. Environ. 130, 245–253.
Jupp, D.L., Culvenor, D., Lovell, J., Newnham, G., Strahler, A., Woodcock, C., 2009. Estimating forest LAI profiles and structural parameters using a ground-based laser called 'Echidna®. Tree Physiol. 29, 171–181.
Kattge, J., Diaz, S., Lavorel, S., Prentice, I.C., Leadley, P., Bönisch, G., Garnier, E., Westoby, M., Reich, P.B., Wright, I.J., 2011. TRY–a global database of plant traits. Glob. Change Biol. 17, 2905–2935.
Korhonen, L., Korpela, I., Heiskanen, J., Maltamo, M., 2011. Airborne discrete-return LIDAR data in the estimation of vertical canopy cover, angular canopy closure and leaf area index. Remote Sens. Environ. 115, 1065–1080.
Kull, O., Broadmeadow, M., Kruijt, B., Meir, P., 1999. Light distribution and foliage structure in an oak canopy. Trees-Struct. Funct. 14, 55–64.
Kuusk, A., 2001. A two-layer canopy reflectance model. J. Quant. Spectrosc. Radiat. Transfer 71, 1–9.
Lang, A., 1973. Leaf orientation of a cotton plant. Agric. Meteorol. 11, 37–51.
Lemeur, R., Blad, B.L., 1975. A critical review of light models for estimating the shortwave radiation regime of plant canopies. Developments in Agricultural and Managed Forest Ecology, Elsevier, pp. 255-286.
Li, Y., Su, Y., Hu, T., Xu, G., Guo, Q., 2018. Retrieving 2-D leaf angle distributions for deciduous trees from terrestrial laser scanner data. IEEE Trans. Geosci. Remote Sens. 1–11.
Liang, X., Hyyppä, J., Kaartinen, H., Lehtomäki, M., Pyörälä, J., Pfeifer, N., Holopainen, M., Brolly, G., Francesco, P., Hackenberg, J., 2018. International benchmarking of terrestrial laser scanning approaches for forest inventories. ISPRS J. Photogramm. Remote Sens. 144, 137–179.
Liu, J., Skidmore, A.K., Heurich, M., Wang, T., 2017. Significant effect of topographic normalization of airborne LiDAR data on the retrieval of plant area index profile in mountainous forests. ISPRS J. Photogramm. Remote Sens. 132, 77–87.
Liu, J., Skidmore, A.K., Jones, S., Wang, T., Heurich, M., Zhu, X., Shi, Y., 2018. Large off-nadir scan angle of airborne LiDAR can severely affect the estimates of forest structure metrics. ISPRS J. Photogramm. Remote Sens. 136, 13–25.
Ma, L., Zheng, G., Eitel, J.U., Moskal, L.M., He, W., Huang, H., 2016. Improved salient feature-based approach for automatically separating photosynthetic and non-photosynthetic components within terrestrial lidar point cloud data of forest canopies. IEEE Trans. Geosci. Remote Sens. 54, 679–696.
McMillen, G.G., McClendon, J.H., 1979. Leaf angle: an adaptive feature of sun and shade leaves. Bot. Gaz. 140, 437–442.
McNeil, B.E., Pisek, J., Lepisk, H., Flamenco, E.A., 2016. Measuring leaf angle distribution in broadleaf canopies using UAVs. Agric. For. Meteorol. 218, 204–208.
Melgani, F., Bruzzone, L., 2004. Classification of hyperspectral remote sensing images with support vector machines. IEEE Trans. Geosci. Remote Sens. 42, 1778–1790.
Muller-Linow, M., Pinto-Espinosa, F., Scharr, H., Rascher, U., 2015. The leaf angle distribution of natural plant populations: assessing the canopy with a novel software tool. Plant Methods 11.
Niinemets, Ü., 2010. A review of light interception in plant stands from leaf to canopy in different plant functional types and in species with varying shade tolerance. Ecol. Res. 25, 693–714.
Norman, J.M., Campbell, G.S., 1989. Canopy structure. Plant physiological ecology. Springer. pp. 301–325.
Ollinger, S., 2011. Sources of variability in canopy reflectance and the convergent properties of plants. New Phytologist 189, 375–394.
Pearcy, R.W., Valladares, F., Wright, S.J., De Paulis, E.L., 2004. A functional analysis of the crown architecture of tropical forest Psychotria species: do species vary in light capture efficiency and consequently in carbon gain and growth? Oecologia 139, 163–177.
Pfennigbauer, M., Ullrich, A., 2010. Improving quality of laser scanning data acquisition through calibrated amplitude and pulse deviation measurement. Laser Radar Technol. Appl. Xv, 7684.
Pisek, J., Ryu, Y., Alikas, K., 2011. Estimating leaf inclination and G-function from leveled digital camera photography in broadleaf canopies. Trees 25, 919–924.
Pisek, J., Sonnentag, O., Richardson, A.D., Mõttus, M., 2013. Is the spherical leaf inclination angle distribution a valid assumption for temperate and boreal broadleaf tree species? Agric. For. Meteorol. 169, 186–194.
Planchais, I., Pontailler, J.Y., 1999. Validity of leaf areas and angles estimated in a beech forest from analysis of gap frequencies, using hemispherical photographs and a plant canopy analyzer. Ann. Forest Sci. 56, 1–10.
Raabe, K., Pisek, J., Sonnentag, O., Annuk, K., 2015. Variations of leaf inclination angle distribution with height over the growing season and light exposure for eight broadleaf tree species. Agric. For. Meteorol. 214, 2–11.
Raumonen, P., Kaasalainen, M., Åkerblom, M., Kaasalainen, S., Kaartinen, H., Vastaranta, M., Holopainen, M., Disney, M., Lewis, P., 2013. Fast automatic precision tree models from terrestrial laser scanner data. Remote Sens. 5, 491–520.
Richardson, J.J., Moskal, L.M., Kim, S.-H., 2009. Modeling approaches to estimate effective leaf area index from aerial discrete-return LIDAR. Agric. For. Meteorol. 149, 1152–1160.
Ross, J., 1981. The Radiation Regime and Architecture of Plant Stands. Springer Science & Business Media.
Ryu, Y., Baldocchi, D.D., Kobayashi, H., Ingen, C., Li, J., Black, T.A., Beringer, J., Gorsel, E., Knohl, A., Law, B.E., 2011. Integration of MODIS land and atmosphere products with a coupled-process model to estimate gross primary productivity and evapotranspiration from 1 km to global scales. Glob. Biogeochem. Cycles 25.
Ryu, Y., Sonnentag, O., Nilson, T., Vargas, R., Kobayashi, H., Wenk, R., Baldocchi, D.D., 2010. How to quantify tree leaf area index in an open savanna ecosystem: a multi-instrument and multi-model approach. Agric. For. Meteorol. 150, 63–76.
Shell, G., Lang, A., Sale, P., 1974. Quantitative measures of leaf orientation and heliotropic response in sunflower, bean, pepper and cucumber. Agric. Meteorol. 13, 25–37.
Silveyra Gonzalez, R., Latifi, H., Weinacker, H., Dees, M., Koch, B., Heurich, M., 2018. Integrating LiDAR and high-resolution imagery for object-based mapping of forest habitats in a heterogeneous temperate forest landscape. Int. J. Remote Sens. 1–26.
Sinoquet, H., Stephan, J., Sonohat, G., Lauri, P., Monney, P., 2007. Simple equations to estimate light interception by isolated trees from canopy structure features: assessment with three-dimensional digitized apple trees. New Phytologist. 175, 94–106.
Sinoquet, H., Thanisawanyangkura, S., Mabrouk, H., Kasemsap, P., 1998. Characterization of the light environment in canopies using 3D digitising and image processing. Ann. Bot. 82, 203–212.
Stark, S.C., Enquist, B.J., Saleska, S.R., Leitold, V., Schietti, J., Longo, M., Alves, L.F., Camargo, P.B., Oliveira, R.C., 2015. Linking canopy leaf area and light environments with tree size distributions to explain Amazon forest demography. Ecol. Lett. 18, 636–645.
Tang, H., Brolly, M., Zhao, F., Strahler, A.H., Schaaf, C.L., Ganguly, S., Zhang, G., Dubayah, R., 2014. Deriving and validating Leaf Area Index (LAI) at multiple spatial scales through lidar remote sensing: a case study in Sierra National Forest, CA. Remote Sens. Environ. 143, 131–141.
Tang, H., Dubayah, R., 2017. Light-driven growth in Amazon evergreen forests explained by seasonal variations of vertical canopy structure. Proceedings of the National Academy of Sciences, 201616943.
Tang, H., Dubayah, R., Swatantran, A., Hofton, M., Sheldon, S., Clark, D.B., Blair, B., 2012. Retrieval of vertical LAI profiles over tropical rain forests using waveform lidar at La Selva, Costa Rica. Remote Sens. Environ. 124, 242–250.
Tol, C., Verhoef, W., Timmermans, J., Verhoef, A., Su, Z., 2009. An integrated model of soil-canopy spectral radiances, photosynthesis, fluorescence, temperature and energy balance. Biogeosciences 6, 3109–3129.
Utsugi, H., Araki, M., Kawasaki, T., Ishizuka, M., 2006. Vertical distributions of leaf area and inclination angle, and their relationship in a 46-year-old *Chamaecyparis obtusa* stand. For. Ecol. Manage. 225, 104–112.
Valladares, F., Gianoli, E., Gómez, J.M., 2007. Ecological limits to plant phenotypic plasticity. New Phytologist 176, 749–763.
Wagner, S., Hagemeier, M., 2006. Method of segmentation affects leaf inclination angle estimation in hemispherical photography. Agric. For. Meteorol. 139, 12–24.
Weiss, M., Baret, F., Smith, G., Jonckheere, I., Coppin, P., 2004. Review of methods for in situ leaf area index (LAI) determination: Part II. Estimation of LAI, errors and sampling. Agric. For. Meteorol. 121, 37–53.
Welles, J.M., 1990. Some indirect methods of estimating canopy structure. Remote Sens. Rev. 5, 31–43.
Wilkes, P., Jones, S.D., Suarez, L., Haywood, A., Woodgate, W., Soto-Berelov, M., Mellor, A., Skidmore, A.K., 2015. Understanding the effects of ALS pulse density for metric retrieval across diverse forest types. Photogramm. Eng. Remote Sens. 81, 625–635.
Wilkes, P., Lau, A., Disney, M., Calders, K., Burt, A., de Tanago, J.G., Bartholomeus, H., Brede, B., Herold, M., 2017. Data acquisition considerations for terrestrial laser scanning of forest plots. Remote Sens. Environ. 196, 140–153.
Wirth, R., Weber, B., Ryel, R.J., 2001. Spatial and temporal variability of canopy structure in a tropical moist forest. Acta Oecologica 22, 235–244.
Xiao, Q., McPherson, E.G., Ustin, S.L., Grismer, M.E., 2000. A new approach to modeling tree rainfall interception. J. Geophys. Res.: Atmos. 105, 29173–29188.
Yang, P., Verhoef, W., Van Der Tol, C., 2017. The mSCOPE model: a simple adaptation to the SCOPE model to describe reflectance, fluorescence and photosynthesis of vertically heterogeneous canopies. Remote Sens. Environ. 201, 1–11.
Zhao, K.G., Garcia, M., Liu, S., Guo, Q.H., Chen, G., Zhang, X.S., Zhou, Y.Y., Meng, X.L., 2015. Terrestrial lidar remote sensing of forests: maximum likelihood estimates of canopy profile, leaf area index, and leaf angle distribution. Agric. For. Meteorol. 209, 100–113.
Zheng, G., Moskal, L.M., 2012. Leaf orientation retrieval from terrestrial laser scanning (TLS) data. IEEE Trans. Geosci. Remote Sens. 50, 3970–3979.
Zhu, X., Skidmore, A.K., Darvishzadeh, R., Niemann, K.O., Liu, J., Shi, Y., Wang, T., 2018. Foliar and woody materials discriminated using terrestrial LiDAR in a mixed natural forest. Int. J. Appl. Earth Observ. Geoinform. 64, 43–50.
Zhu, X., Wang, T., Skidmore, A.K., Darvishzadeh, R., Niemann, K.O., Liu, J., 2017. Canopy leaf water content estimated using terrestrial LiDAR. Agric. For. Meteorol. 232, 152–162.